

Constraint Propagation of C^2 -adjusted Formulation II — Another Recipe for Robust BSSN Evolution System —

Takuya Tsuchiya* and Gen Yoneda

Department of Mathematical Sciences, Waseda University, Okubo, Shinjuku, Tokyo, 169-8555, Japan

Hisa-aki Shinkai

*Faculty of Information Science and Technology, Osaka Institute of Technology,
1-79-1 Kitayama, Hirakata, Osaka 573-0196, Japan*

*Computational Astrophysics Laboratory, Institute of Physical & Chemical
Research (RIKEN), Hirosawa, Wako, Saitama, 351-0198 Japan*

(Dated: September 28, 2011)

To obtain an evolution system robust against the violation of constraints, we present a new set of evolution systems based on the so-called Baumgarte-Shapiro-Shibata-Nakamura (BSSN) equations. The idea is to add functional derivatives of the norm of constraints, C^2 , to the evolution equations, which was proposed by Fiske (2004) and was applied to the ADM formulation in our previous study. We derive the constraint propagation equations, discuss the behavior of constraint damping, and present the results of numerical tests using the gauge-wave and polarized Gowdy wave spacetimes. The construction of the C^2 -adjusted system is straightforward. However, in BSSN, there are two kinetic constraints and three algebraic constraints; thus, the definition of C^2 is a matter of concern. By analyzing constraint propagation equations, we conclude that C^2 should include all the constraints, which is also confirmed numerically. By tuning the parameters, the lifetime of the simulations can be increased to 2-10 times longer than that of standard BSSN evolutions.

PACS numbers: 04.25.D-

I. INTRODUCTION

When solving the Einstein equations numerically, the standard way is to split the spacetime into space and time. The most fundamental decomposition of the Einstein equations is the Arnowitt-Deser-Misner (ADM) formulation [1, 2]. However, it is well known that in long-term evolutions in strong gravitational fields such as the coalescences of binary neutron stars and/or black holes, simulations with the ADM formulation are unstable and are often interrupted before producing physically interesting results. Finding more robust and stable formulations is known as the “formulation problem” in numerical relativity [3–5].

Many formulations have been proposed in the last two decades. The most commonly used sets of evolution equations among numerical relativists are the so-called Baumgarte-Shapiro-Shibata-Nakamura (BSSN) formulation [6, 7], the generalized harmonic (GH) formulation [8, 9], the Kidder-Scheel-Teukolsky (KST) formulation [10], and the Z4 formulation [11, 12] (we here cite [13, 14] for applications of the BSSN formulation, [15] for the GH formulation, [16] for the KST formulation, and [17] for the Z4 formulation).

The above modern formulations all include the technique of “constraint damping”, which attempts to control the violations of constraints by adding the constraint terms to evolution equations. Using this technique, more stable and accurate systems are realized (for examples of

research on this technique, see [18, 19]). This technique is simply an adjustment of the original system.

In [20–22], two of the authors systematically investigated how the adjusted terms change the original systems by calculating the constraint propagation equations. The authors suggested some effective adjustments for the BSSN formulation under the name “adjusted BSSN formulation” [22]. The actual constraint damping effect was confirmed by numerical tests [23].

Fiske proposed a method of adjusting the original evolution system using the norm of the constraints, C^2 , [24]. We call such a system a “ C^2 -adjusted system.” The new evolution equations cause the constraints to evolve towards their decay if the coefficient parameters of the adjusted terms are set as appropriate positive values. Fiske reported the damping effect of the constraint violations for the Maxwell system [24] and for the linearized ADM and BSSN formulations [25]. He also reported the limitation of the magnitude of the coefficient parameters of the adjusted terms.

In [26], we applied the C^2 -adjusted system to the (full) ADM formulation and performed some numerical tests. We confirmed that the violations of the constraints are less than those in the original system. We also reported the differences in the effective range of the coefficient parameters of the adjusted terms for the evolution equations of three-metric and extrinsic curvature.

In this article, we apply the C^2 -adjusted system to the (full) BSSN formulation and derive the constraint propagation equations in flat space. We perform some numerical tests and compare three types of BSSN formulations: the standard BSSN formulation, the \tilde{A} -adjusted BSSN

* tsuchiya@akane.waseda.jp

formulation, and the C^2 -adjusted BSSN formulation. We use the gauge-wave and polarized Gowdy wave testbeds, which are the test problems as is known to apples-with-apples testbeds [27]. Since the models are precisely fixed up to the gauge conditions, boundary conditions, and technical parameters, testbeds are widely used for comparisons between formulations [23, 28, 29].

The structure of this article is as follows. We review the ideas of adjusted systems and the C^2 -adjusted system in Sec.II. In Sec.III, we review the standard and adjusted BSSN formulations and derive the C^2 -adjusted BSSN formulation. In Sec.IV, we perform some numerical tests in the gauge-wave and polarized Gowdy wave testbeds to show the damping effect of the constraint violations. We summarize this article in Sec.V. In this article, we only consider vacuum spacetime, but the inclusion of matter is straightforward.

II. IDEAS OF ADJUSTED SYSTEMS AND C^2 -ADJUSTED SYSTEMS

A. Idea of adjusted systems

Suppose we have dynamical variables u^i that evolve with the evolution equations

$$\partial_t u^i = f(u^i, \partial_j u^i, \dots), \quad (2.1)$$

and suppose also that the system has the (first class) constraint equations

$$C^a(u^a, \partial_j u^a, \dots) \approx 0. \quad (2.2)$$

We can then predict how the constraints are preserved by evaluating the constraint propagation equations

$$\partial_t C^a = g(C^a, \partial_i C^a, \dots), \quad (2.3)$$

which measure the violation behavior of constraints C^a in time evolution. Equation (2.3) is theoretically weakly zero, i.e., $\partial_t C^a \approx 0$, since the system is supposed to be first class. However, free numerical evolution with discretized grids introduces a constraint violation, at least at the level of truncation error, which sometimes grows and stops the simulations. The unstable feature of ADM evolution can be understood on the basis of this analysis [15].

Such features of the constraint propagation equations, (2.3), change when we modify the original evolution equations. Suppose we add the constraint terms to the right-hand-side of (2.1) as

$$\partial_t u^i = f(u^i, \partial_j u^i, \dots) + F(C^a, \partial_j C^a, \dots), \quad (2.4)$$

where $F(C^a, \dots) \approx 0$ in principle but not exactly zero in numerical evolutions. Equation (2.3) will also be modified to

$$\partial_t C^a = g(C^a, \partial_i C^a, \dots) + G(C^a, \partial_i C^a, \dots). \quad (2.5)$$

Therefore, we are able to control $\partial_t C^a$ by making an appropriate adjustment $F(C^a, \partial_j C^a, \dots)$ in (2.4). If $\partial_t C^a < 0$ is realized, then the system has the constraint surface as an attractor.

This technique is also known as a constraint-damping technique. Almost all the current popular formulations used for large-scale numerical simulations include this implementation. The purpose of this article is to find a better way of adjusting the evolution equations to realize $\partial_t C^a \leq 0$.

B. Idea of C^2 -adjusted systems

Fiske [24] proposed a way of adjusting the evolution equations which we call “ C^2 -adjusted systems”;

$$\partial_t u^i = f(u^i, \partial_j u^i, \dots) - \kappa^{ij} \left(\frac{\delta C^2}{\delta u^j} \right), \quad (2.6)$$

where κ^{ij} is a positive-definite constant coefficient and C^2 is the norm of the constraints, which is defined as $C^2 \equiv \int C_a C^a d^3x$. The term $(\delta C^2 / \delta u^j)$ is the functional derivative of C^2 with respect to u^j . The associated constraint propagation equation becomes

$$\partial_t C^2 = h(C^a, \partial_i C^a, \dots) - \int d^3x \left(\frac{\delta C^2}{\delta u^i} \right) \kappa^{ij} \left(\frac{\delta C^2}{\delta u^j} \right). \quad (2.7)$$

The motivation for this adjustment is to naturally obtain the constraint-damping system, $\partial_t C^2 < 0$. If we set κ^{ij} so that the second term on the right-hand side of (2.7) becomes larger than the first term, then $\partial_t C^2$ becomes negative, which indicates that constraint violations are expected to decay to zero. Fiske presented numerical examples for the Maxwell system and the linearized ADM and BSSN formulations, and concluded that this method actually reduces constraint violations as expected. In a previous work [26], we applied the C^2 -adjusted system to the (full) ADM formulation and calculated the constraint propagation equations, then we confirmed that $\partial_t C^2 < 0$ was expected in flat spacetime. We performed numerical tests with the C^2 -adjusted ADM formulation using the gauge-wave and Gowdy wave testbeds, and confirmed that the violations of the constraint are lower than those of the standard ADM formulation. The simulation continued 1.7 times longer than that of the standard ADM formulation with the magnitude of the violations of the constraint less than order $O(10^0)$.

III. APPLICATION TO BSSN FORMULATION

A. Standard BSSN formulation

As the notation [7] of the BSSN system, the dynamical variables $(\varphi, K, \tilde{\gamma}_{ij}, \tilde{A}_{ij}, \tilde{\Gamma}^i)$ are widely used instead of the

variables of the ADM formulation, (γ_{ij}, K_{ij}) , where

$$\varphi \equiv (1/12) \log(\det(\gamma_{ij})), \quad (3.1)$$

$$K \equiv \gamma^{ij} K_{ij}, \quad (3.2)$$

$$\tilde{\gamma}_{ij} \equiv e^{-4\varphi} \gamma_{ij}, \quad (3.3)$$

$$\tilde{A}_{ij} \equiv e^{-4\varphi} (K_{ij} - (1/3)\gamma_{ij}K), \text{ and} \quad (3.4)$$

$$\tilde{\Gamma}^i \equiv \tilde{\gamma}^{mn} \tilde{\Gamma}^i_{mn}. \quad (3.5)$$

The BSSN evolution equations are, then,

$$\partial_t \varphi = -(1/6)\alpha K + (1/6)(\partial_i \beta^i) + \beta^i (\partial_i \varphi), \quad (3.6)$$

$$\partial_t K = \alpha \tilde{A}_{ij} \tilde{A}^{ij} + (1/3)\alpha K^2 - D_i D^i \alpha + \beta^i (\partial_i K), \quad (3.7)$$

$$\begin{aligned} \partial_t \tilde{\gamma}_{ij} = & -2\alpha \tilde{A}_{ij} - (2/3)\tilde{\gamma}_{ij}(\partial_\ell \beta^\ell) \\ & + \tilde{\gamma}_{j\ell}(\partial_i \beta^\ell) + \tilde{\gamma}_{i\ell}(\partial_j \beta^\ell) + \beta^\ell (\partial_\ell \tilde{\gamma}_{ij}), \end{aligned} \quad (3.8)$$

$$\begin{aligned} \partial_t \tilde{A}_{ij} = & \alpha K \tilde{A}_{ij} - 2\alpha \tilde{A}_{i\ell} \tilde{A}^\ell_j + \alpha e^{-4\varphi} R_{ij}^{TF} \\ & - e^{-4\varphi} (D_i D_j \alpha)^{TF} - (2/3)\tilde{A}_{ij}(\partial_\ell \beta^\ell) \\ & + (\partial_i \beta^\ell) \tilde{A}_{j\ell} + (\partial_j \beta^\ell) \tilde{A}_{i\ell} + \beta^\ell (\partial_\ell \tilde{A}_{ij}), \end{aligned} \quad (3.9)$$

$$\begin{aligned} \partial_t \tilde{\Gamma}^i = & 2\alpha \{6(\partial_j \varphi) \tilde{A}^{ij} + \tilde{\Gamma}^i_{j\ell} \tilde{A}^{j\ell} - (2/3)\tilde{\gamma}^{ij}(\partial_j K)\} \\ & - 2(\partial_j \alpha) \tilde{A}^{ij} + (2/3)\tilde{\Gamma}^i(\partial_j \beta^j) + (1/3)\tilde{\gamma}^{ij}(\partial_\ell \partial_j \beta^\ell) \\ & + \beta^\ell (\partial_\ell \tilde{\Gamma}^i) - \tilde{\Gamma}^j(\partial_j \beta^i) + \tilde{\gamma}^{j\ell}(\partial_j \partial_\ell \beta^i), \end{aligned} \quad (3.10)$$

where TF denotes the trace-free part. The Ricci tensor in the BSSN system is normally calculated as

$$R_{ij} \equiv \tilde{R}_{ij} + R_{ij}^\varphi, \quad (3.11)$$

where

$$\begin{aligned} \tilde{R}_{ij} \equiv & \tilde{\gamma}_{n(i} \partial_j) \tilde{\Gamma}^n + \tilde{\gamma}^{\ell m} (2\tilde{\Gamma}^k_{\ell(i} \tilde{\Gamma}_{j)km} + \tilde{\Gamma}_{n\ell j} \tilde{\Gamma}^n_{im}) \\ & - (1/2)\tilde{\gamma}^{m\ell} \tilde{\gamma}_{ij,ml} + \tilde{\Gamma}^n \tilde{\Gamma}_{(ij)n}, \end{aligned} \quad (3.12)$$

$$\begin{aligned} R_{ij}^\varphi \equiv & -2\tilde{D}_i \tilde{D}_j \varphi + 4(\tilde{D}_i \varphi)(\tilde{D}_j \varphi) - 2\tilde{\gamma}_{ij} \tilde{D}_m \tilde{D}^m \varphi \\ & - 4\tilde{\gamma}_{ij}(\tilde{D}^m \varphi)(\tilde{D}_m \varphi). \end{aligned} \quad (3.13)$$

The BSSN system has five constraint equations. The ‘‘kinematic’’ constraint equations, which are the Hamiltonian constraint equation and the momentum constraint equations (\mathcal{H} -constraint and \mathcal{M} -constraint, hereafter), are expressed in terms of the BSSN basic variables as

$$\begin{aligned} \mathcal{H} \equiv & e^{-4\varphi} \tilde{R} - 8e^{-4\varphi} (\tilde{D}_i \tilde{D}^i \varphi + (\tilde{D}^m \varphi)(\tilde{D}_m \varphi)) \\ & + (2/3)K^2 - \tilde{A}_{ij} \tilde{A}^{ij} - (2/3)\mathcal{A}K \approx 0, \end{aligned} \quad (3.14)$$

$$\begin{aligned} \mathcal{M}_i \equiv & -(2/3)\tilde{D}_i K + 6(\tilde{D}_j \varphi) \tilde{A}^j_i + \tilde{D}_j \tilde{A}^j_i \\ & - 2(\tilde{D}_i \varphi)\mathcal{A} \approx 0, \end{aligned} \quad (3.15)$$

respectively, where \tilde{D}_i is the covariant derivative associated with $\tilde{\gamma}_{ij}$ and $\tilde{R} = \tilde{\gamma}^{ij} \tilde{R}_{ij}$. Because of the introduction of new variables, there are additional ‘‘algebraic’’ constraint equations:

$$\mathcal{G}^i \equiv \tilde{\Gamma}^i - \tilde{\gamma}^{j\ell} \tilde{\Gamma}^i_{j\ell} \approx 0, \quad (3.16)$$

$$\mathcal{A} \equiv \tilde{A}^{ij} \tilde{\gamma}_{ij} \approx 0, \quad (3.17)$$

$$\mathcal{S} \equiv \det(\tilde{\gamma}_{ij}) - 1 \approx 0, \quad (3.18)$$

which we call the \mathcal{G} -, \mathcal{A} -, and \mathcal{S} -constraints, respectively, hereafter. If the algebraic constraint equations, (3.16)-(3.18), are not satisfied, the BSSN formulation and ADM formulation are not equivalent mathematically.

B. C^2 -adjusted BSSN formulation

The C^2 -adjusted BSSN evolution equations are formally written as

$$\partial_t \varphi = (3.6) - \lambda_\varphi \left(\frac{\delta C^2}{\delta \varphi} \right), \quad (3.19)$$

$$\partial_t K = (3.7) - \lambda_K \left(\frac{\delta C^2}{\delta K} \right), \quad (3.20)$$

$$\partial_t \tilde{\gamma}_{ij} = (3.8) - \lambda_{\tilde{\gamma}_{ijmn}} \left(\frac{\delta C^2}{\delta \tilde{\gamma}_{mn}} \right), \quad (3.21)$$

$$\partial_t \tilde{A}_{ij} = (3.9) - \lambda_{\tilde{A}_{ijmn}} \left(\frac{\delta C^2}{\delta \tilde{A}_{mn}} \right), \quad (3.22)$$

$$\partial_t \tilde{\Gamma}^i = (3.10) - \lambda_{\tilde{\Gamma}^i}^{ij} \left(\frac{\delta C^2}{\delta \tilde{\Gamma}^j} \right), \quad (3.23)$$

where all the coefficients λ_φ , λ_K , $\lambda_{\tilde{\gamma}_{ijmn}}$, $\lambda_{\tilde{A}_{ijmn}}$, and $\lambda_{\tilde{\Gamma}^i}^{ij}$ are positive definite. C^2 is a function of the constraints \mathcal{H} , \mathcal{M}_i , \mathcal{G}^i , \mathcal{A} , and \mathcal{S} , which we set as

$$\begin{aligned} C^2 = & \int (\mathcal{H}^2 + \gamma^{ij} \mathcal{M}_i \mathcal{M}_j + c_G \gamma_{ij} \mathcal{G}^i \mathcal{G}^j \\ & + c_A \mathcal{A}^2 + c_S \mathcal{S}^2) d^3x, \end{aligned} \quad (3.24)$$

where, c_G , c_A , and c_S are Boolean parameters (0 or 1). These three parameters are introduced to prove the necessity of the algebraic constraint terms in (3.24).

The adjusted terms in (3.19)-(3.23) are then written down explicitly, as shown in Appendix A. The constraint propagation equations of this system are also derived for the Minkowskii background, as shown in Appendix B.

Now we discuss the effect of the algebraic constraints. From (B1)-(B5), we see that the constraints affect each others. Also, the constraint propagation equations of the algebraic constraints, (B3)-(B5), include $c_G(\lambda_{\tilde{\gamma}} \Delta \delta^{a_b} - 2\lambda_{\tilde{\Gamma}} \delta^{a_b}) \mathcal{G}^b$, $-6c_A \lambda_{\tilde{A}} \mathcal{A}$, and $-6c_S \lambda_{\tilde{\gamma}} \mathcal{S}$, respectively. These terms contribute to reducing the violations of each constraint if c_G , c_A , and c_S are nonzero. Therefore, we adopt $c_G = c_A = c_S = 1$ in (3.24);

$$C^2 = \int (\mathcal{H}^2 + \gamma^{ij} \mathcal{M}_i \mathcal{M}_j + \gamma_{ij} \mathcal{G}^i \mathcal{G}^j + \mathcal{A}^2 + \mathcal{S}^2) d^3x. \quad (3.25)$$

In Sec.IV, we verify the validity of this decision using numerical examples.

C. \tilde{A} -adjusted BSSN system

In [22], two of the authors reported some examples of adjusted systems for the BSSN formulation. The au-

thors investigated the signatures of eigenvalues of the coefficient matrix of the constraint propagation equations, and concluded three of the examples to be the best candidates for the adjustment. The actual numerical tests were performed later [23] using the gauge-wave, linear-wave, and polarized Gowdy wave testbeds. The most robust system among the three examples for these three testbeds was the \tilde{A} -adjusted BSSN formulation, which replaces (3.9) in the standard BSSN system with

$$\partial_t \tilde{A}_{ij} = (3.9) + \kappa_A \alpha \tilde{D}_{(i} \mathcal{M}_{j)}, \quad (3.26)$$

where κ_A is a constant. If κ_A is set as positive, the violations of the constraints are expected to be damped in flat spacetime [22]. We also use the \tilde{A} -adjusted BSSN system for comparison in the following numerical tests.

IV. NUMERICAL EXAMPLES

We test the proposed adjusted systems (C^2 -adjusted BSSN, \tilde{A} -adjusted BSSN, and the standard BSSN) in numerical evolutions using the gauge-wave and polarized Gowdy wave spacetimes, which are the standard tests for comparisons of formulations in numerical relativity, and are known as apples-with-apples testbeds [27]. We also performed the linear-wave testbed but the violations of the constraint were negligible; thus, we employ only the above two testbeds in this article. These tests have been used by several groups and were reported in the same manner (e.g., [23, 28–30]).

For simplicity, we set the coefficient parameters in (3.21)-(3.23) to $\lambda_{\tilde{\gamma}}^{ijmn} = \lambda_{\tilde{\gamma}} \delta_{im} \delta_{jn}$, $\lambda_{\tilde{A}}^{ijmn} = \lambda_{\tilde{A}} \delta_{im} \delta_{jn}$, and $\lambda_{\tilde{\Gamma}}^{ij} = \lambda_{\tilde{\Gamma}} \delta^{ij}$ with non-negative coefficient constant parameters $\lambda_{\tilde{\gamma}}$, $\lambda_{\tilde{A}}$, and $\lambda_{\tilde{\Gamma}}$. Our code passes the convergence test with second-order accuracy. We list the figures in this article in Table I.

A. Gauge-wave Testbed

1. Metric and Parameters

The metric of the gauge-wave test is

$$ds^2 = -H dt^2 + H dx^2 + dy^2 + dz^2, \quad (4.1)$$

where

$$H = 1 - A \sin(2\pi(x-t)/d), \quad (4.2)$$

which describes a sinusoidal gauge wave of amplitude A propagating along the x -axis. The nontrivial extrinsic curvature is

$$K_{xx} = -\frac{\pi A}{d} \frac{\cos(\frac{2\pi(x-t)}{d})}{\sqrt{1 - A \sin \frac{2\pi(x-t)}{d}}}. \quad (4.3)$$

Following [27], we chose the numerical domain and parameters as follows:

- Gauge-wave parameters: $d = 1$ and $A = 10^{-2}$.
- Simulation domain: $x \in [-0.5, 0.5]$, $y = z = 0$.
- Grid: $x^n = -0.5 + (n-1/2)dx$ with $n = 1, \dots, 100$, where $dx = 1/100$.
- Time step: $dt = 0.25dx$.
- Boundary conditions: Periodic boundary condition in x -direction and planar symmetry in y - and z -directions.
- Gauge conditions:
$$\partial_t \alpha = -\alpha^2 K, \quad \beta^i = 0. \quad (4.4)$$
- Scheme: second-order iterative Crank-Nicolson.

2. Constraint Violations and Damping of Violations

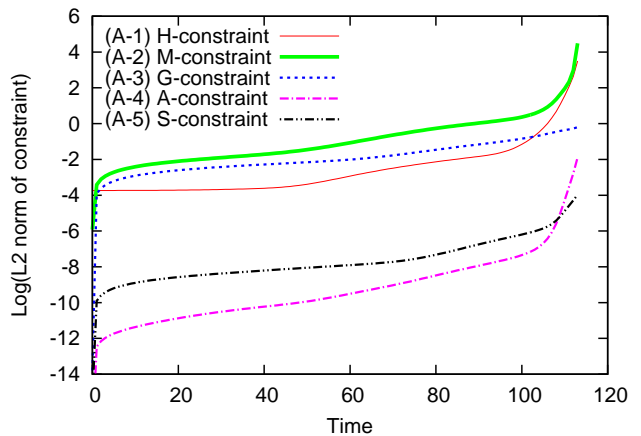


FIG. 1. L2 norm of each constraint in the gauge-wave evolution using the standard BSSN formulation. The vertical axis is the logarithm of the L2 norm of the constraints and the horizontal axis is time. The thin solid line (A-1) is the \mathcal{H} -constraint, the thick solid line (A-2) is the \mathcal{M} -constraint, the dotted line (A-3) is the \mathcal{G} -constraint, the dot-dashed line (A-4) is the \mathcal{A} -constraint, and the two-dot-dashed line (A-5) is the \mathcal{S} -constraint.

Figure 1 shows the violations of five constraint equations \mathcal{H} , \mathcal{M}_i , \mathcal{G}^i , \mathcal{A} , and \mathcal{S} for the gauge-wave evolution using the standard BSSN formulation. The violation of the \mathcal{M} -constraint, line (A-2), is the largest during the evolution, while the violations of both the \mathcal{A} -constraint and \mathcal{S} -constraint are negligible. This is the starting point for improving the BSSN formulation.

Applying the adjustment procedure, the lifetime of the standard BSSN evolution is increased at least 10-fold. In Fig.2, we plot the L2 norm of the constraints, (3.25), of three BSSN formulations: (A) the standard BSSN formulation (3.1)-(3.5), (B) the \tilde{A} -adjusted BSSN formulation

TABLE I. List of figures.

	gauge-wave test §IV A	Gowdy wave test §IV B
(A) (D) standard BSSN (3.1)-(3.5) (constraint propagation, see App. in [22])	Fig.1 norm each Fig.2 norm all	Fig.7 norm each Fig.8 norm all
(B) (E) \tilde{A} -adjusted BSSN (3.1)-(3.3), (3.5) and (3.26) (constraint propagation, see [22])	Fig.2 norm all Fig.3 norm each	Fig.8 norm all
(C) (F) C^2 -adjusted BSSN (3.19)-(3.23) (constraint propagation, see App. B)	Fig.2 norm all Fig.3 norm each Fig.4 correction test Fig.5 (3.19)-(3.23) test Fig.6 (3.25) test	Fig.8 norm all Fig.9 norm each Fig.10 correction test Fig.11 (3.19)-(3.23) test Fig.12 (3.25) test

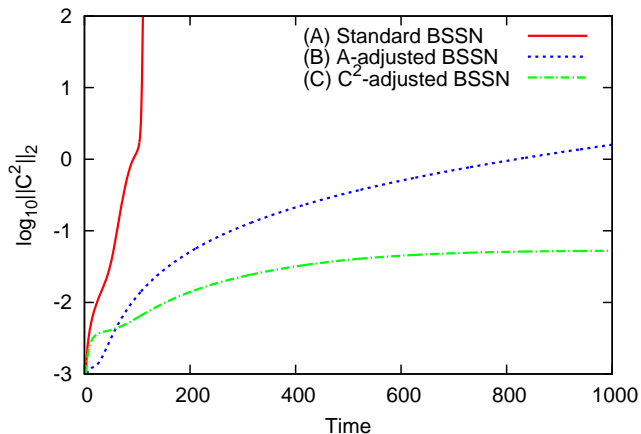


FIG. 2. L2 norm of all the constraints in gauge-wave evolution comparing three BSSN formulations: (A) standard BSSN formulation (solid line), (B) \tilde{A} -adjusted BSSN formulation (dotted line), and (C) C^2 -adjusted BSSN formulation (dot-dashed line). The adopted parameters are $\kappa_A = 10^{-1.6}$ for (B), and $\lambda_\varphi = 10^{-8.5}$, $\lambda_K = 10^{-8.4}$, $\lambda_{\tilde{\gamma}} = 10^{-7.3}$, $\lambda_{\tilde{A}} = 10^{-2.5}$, and $\lambda_{\tilde{\Gamma}} = 10^{-1.8}$ for (C). The violations of C^2 for the \tilde{A} -adjusted BSSN formulation, (B), increase with time and the simulation stops at $t = 1200$, while the violations of C^2 for the C^2 -adjusted BSSN formulation, (C), remain at $O(10^{-1})$ until $t = 1300$ and the simulation stops before $t = 1400$.

(3.1)-(3.3), (3.5), and (3.26), and (C) the C^2 -adjusted BSSN formulation (3.19)-(3.23). We set the parameter of the \tilde{A} -adjusted BSSN formulation to $\kappa_A = 10^{-1.6}$ and the parameters of the C^2 -adjusted BSSN formulation to $\lambda_\varphi = 10^{-8.5}$, $\lambda_K = 10^{-8.4}$, $\lambda_{\tilde{\gamma}} = 10^{-7.3}$, $\lambda_{\tilde{A}} = 10^{-2.5}$, and $\lambda_{\tilde{\Gamma}} = 10^{-1.8}$ to minimize C^2 at $t = 1000$. The figure shows the damping of the constraint violations for the \tilde{A} -adjusted BSSN formulation [line (B)] and the C^2 -adjusted BSSN formulation [line (C)] in contrast to the standard BSSN formulation [line (A)]. Line (B) monotonically increases, while line (C) has an L2 norm remaining at a level $\leq O(10^{-1})$ after $t = 600$.

The violation of C^2 for the \tilde{A} -adjusted BSSN formulation is the smallest among the three formulations until

$t = 50$, after which that for the C^2 -adjusted BSSN formulation is the smallest.

To observe the behavior of each violation of the constraint for the two adjusted BSSN formulations, we plot the norm of each constraint equation in Fig.3. We see that the violations of the \mathcal{M} -constraint for the two adjusted BSSN formulations, (B-2) and (C-2), are less than those of the standard BSSN formulation in Fig.1. This is the main consequence of the two adjusted BSSN formulations.

In the two panels in Fig.3, we see that the dominant violation changes from the \mathcal{M} -constraint to the \mathcal{S} -constraint as the evolution continues. Before $t = 100$, line (B-2) is lower than line (C-2). After that, line (C-5) is lower than line (B-5). This explains the intersection of lines (B) and (C) at $t = 50$ in Fig.2. Since line (B-5) overlaps with line (B) in Fig.2 after $t = 100$ and line (C-5) overlaps with line (C) in Fig.2 after $t = 500$, the reduction of the violations of the \mathcal{S} -constraint is the key to reducing C^2 for the C^2 -adjusted BSSN formulation.

In panel (b), we see that all the violations of the constraints are better controlled than in panel (a), and we thus conclude that the C^2 -adjusted BSSN formulation is more robust against the violation of constraints than the \tilde{A} -adjusted BSSN formulation.

The violations of the \mathcal{A} -constraint and \mathcal{S} -constraint are larger than those in Fig.1. From (B4) and (C4), the violation of the \mathcal{A} -constraint is triggered by the \mathcal{M} -constraint and \mathcal{A} -constraint. The increase in the violations of the \mathcal{A} -constraint is caused by the term $2\lambda_{\tilde{A}}\delta^{ij}(\partial_i\mathcal{M}_j)$, since the other adjusted term, $-6c_A\lambda_{\tilde{A}}\mathcal{A}$, contributes to reducing the violations of the \mathcal{A} -constraint. Similarly, in (B5) and (C5), the violation of the \mathcal{S} -constraint is triggered by only the \mathcal{A} -constraint since the magnitude of $\lambda_{\tilde{\gamma}}$ is negligible. Therefore, the increase in the violations of the \mathcal{S} -constraint is due to the increase in the violations of the \mathcal{A} -constraint.

The lower positions of lines (B-2) and (C-2) in Fig.3 than line (A-2) in Fig.1 is explained by the terms $\lambda_{\tilde{A}}\Delta\mathcal{M}_a$ in (B2) and $(1/2)\kappa_A\Delta\mathcal{M}_i$ in (B7), respectively, since these terms contribute to reducing the violations of the \mathcal{M} -constraint.

From (A1) and (A3), it can be seen that the adjusted

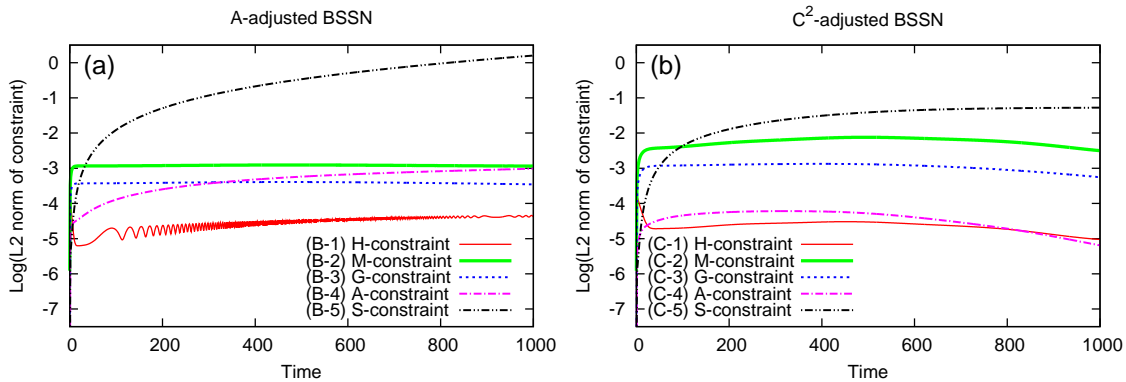


FIG. 3. L2 norm of each constraint in the gauge-wave evolution using the \tilde{A} -adjusted BSSN formulation [panel (a)] and C^2 -adjusted BSSN formulation [panel (b)]. The thin solid lines (B-1) and (C-1) are the \mathcal{H} -constraint, the thick solid lines (B-2) and (C-2) are the \mathcal{M} -constraint, the dotted lines (B-3) and (C-3) are the \mathcal{G} -constraint, the dot-dashed lines (B-4) and (C-4) are the \mathcal{A} -constraint, and the two-dot-dashed lines (B-5) and (C-5) are the \mathcal{S} -constraint. The parameters κ_A , λ_φ , λ_K , $\lambda_{\tilde{\gamma}}$, $\lambda_{\tilde{A}}$, and $\lambda_{\tilde{\Gamma}}$ are the same as those in Fig.2. In both panels, we see that the violations of the \mathcal{H} -constraint (B-1) and (C-1), the \mathcal{M} -constraint (B-2) and (C-2), and the \mathcal{G} -constraint (B-3) and (C-3) are less than those for the standard BSSN formulation in Fig.1. However, the violations of the \mathcal{A} -constraint (B-4) and (C-4) and the \mathcal{S} -constraint (B-5) and (C-5) are larger. Line (B-5) overlaps with line (B) in Fig.2 after $t = 100$, and line (C-5) overlaps with line (C) in Fig.1 after $t = 500$.

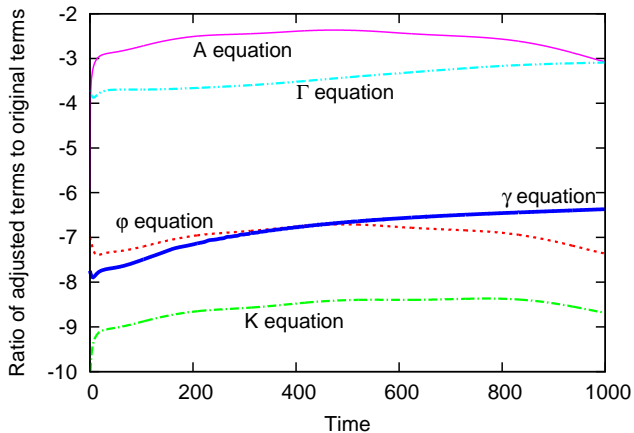


FIG. 4. L2 norm of (adjusted terms)/(original terms) of each evolution equation for the C^2 -adjusted BSSN formulation, (3.19)-(3.23), in the gauge-wave test. We see that the largest ratio is that for the evolution equation of \tilde{A}_{ij} . The corrections to the φ , K , and $\tilde{\gamma}_{ij}$ evolution equations are reasonably small.

terms of the evolution equations of φ and $\tilde{\gamma}_{ij}$ for the C^2 -adjusted BSSN formulation include a second-order derivative of the \mathcal{H} -constraint. This means that these evolution equations include fourth-order derivative terms of the dynamical variables. To investigate the magnitudes of the adjusted terms, we show the ratio of the L2 norm of the original terms to that of the additional terms in the evolution equations in Fig.4. We see that the magnitudes of the adjusted terms of φ and $\tilde{\gamma}_{ij}$ are reasonably small. Therefore, the characteristic of the C^2 -adjusted

evolution system cannot be changed from hyperbolic to parabolic by adjusting the procedures.

In the simulations with the C^2 -adjusted BSSN formulation, the constraint with the largest violation is the \mathcal{S} -constraint. The \mathcal{S} -constraint depends only on the dynamical variables $\tilde{\gamma}_{ij}$. To control the \mathcal{S} -constraint directly, there is no other choice than setting $\lambda_{\tilde{\gamma}}$ to an appropriate value, as can be seen from (B5). However, we must set $\lambda_{\tilde{\gamma}}$ to a value as small as possible since the adjusted term of $\tilde{\gamma}_{ij}$ includes higher derivatives of $\tilde{\gamma}_{ij}$. Therefore, it is difficult to control the \mathcal{S} -constraint, and we have not yet found an appropriate set of parameters.

3. Damping Effect of each Adjusted Term in C^2 -adjusted BSSN Formulation

To observe the differences in the effect of the reduction of the violations of constraints for each of the adjusted terms, we compared evolutions for a set of equations applying only one of the adjusted terms. As previously mentioned, the reduction of the \mathcal{M} -constraint is the key to improving constraint damping in gauge-wave space-time at an earlier time (approximately $t = 100$). From (B2), we see that the adjusted terms of K and \tilde{A}_{ij} directly affect the \mathcal{M} -constraint. The left panel in Fig.5 shows the norm of C^2 with $\lambda_{\tilde{A}} \neq 0$ and $\lambda_\varphi = \lambda_K = \lambda_{\tilde{\gamma}} = \lambda_{\tilde{\Gamma}} = 0$. The right panel shows C^2 with $\lambda_K \neq 0$ and $\lambda_\varphi = \lambda_{\tilde{\gamma}} = \lambda_{\tilde{A}} = \lambda_{\tilde{\Gamma}} = 0$. In both cases, we confirm that the violation of constraints is dominated by that of the \mathcal{M} -constraint. In the left panel, we see that the case of $\lambda_{\tilde{A}} = 10^{-3}$ is the best-controlled evolution, while in the right panel we see that the standard BSSN evolution minimizes the violation of constraints. The latter indicates

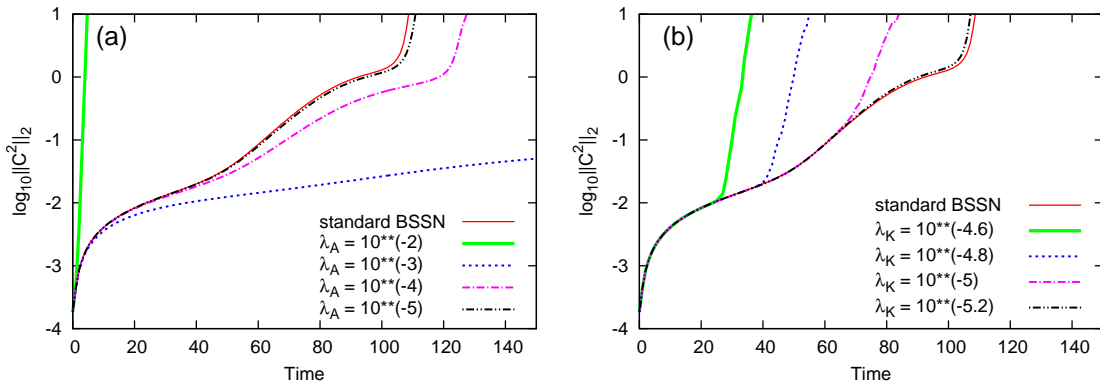


FIG. 5. Sensitivity of adjusting parameters for the C^2 -adjusted BSSN formulation, (3.19)-(3.23). The left panel shows the case when $\lambda_{\bar{A}} \neq 0$ and the other parameters are zero. The right panel shows the case when $\lambda_{\bar{\gamma}} \neq 0$ and the other parameters are zero. We see that if we set $\lambda_{\bar{A}}$ to an appropriate value such as $\lambda_{\bar{A}} = 10^{-3}$, then the violation of C^2 decreases ideally. However, the violation of C^2 is larger than that for the standard BSSN formulation if only λ_K is nonzero.

that the adjustment to the K -equation, (3.20), does not contribute to reducing any of the constraint violations if it is the only adjustment implemented.

B. Gowdy wave Testbed

1. Metric and Parameters

The metric of the polarized Gowdy wave is given by

$$ds^2 = t^{-1/2} e^{\lambda/2} (-dt^2 + dx^2) + t(e^P dy^2 + e^{-P} dz^2), \quad (4.5)$$

where P and λ are functions of x and t . The forward direction of the time coordinate t corresponds to the expanding universe, and $t = 0$ corresponds to the cosmological singularity.

For simple forms of the solutions, P and λ are given by

$$\begin{aligned} P &= J_0(2\pi t) \cos(2\pi x), \\ \lambda &= -2\pi t J_0(2\pi t) J_1(2\pi t) \cos^2(2\pi x) + 2\pi^2 t^2 [J_0^2(2\pi t) \\ &\quad + J_1^2(2\pi t)] - (1/2) \{ (2\pi)^2 [J_0^2(2\pi) + J_1^2(2\pi)] \\ &\quad - 2\pi J_0(2\pi) J_1(2\pi) \}, \end{aligned} \quad (4.7)$$

where J_n is the Bessel function.

Following [27], a new time coordinate τ , which satisfies harmonic slicing, is obtained by the coordinate transformation

$$t(\tau) = k e^{c\tau}, \quad (4.8)$$

where k and c are arbitrary constants. We also follow [27] by setting k , c , and the initial time t_0 as

$$k \sim 9.67076981276405, \quad c \sim 0.002119511921460, \quad (4.9)$$

$$t_0 = 9.87532058290982, \quad (4.10)$$

so that the lapse function in the new time coordinate is unity and $t = \tau$ at the initial time.

We also use the following parameters specified in [27].

4. Damping Effect of Algebraic Constraints

In Sec.III B, we started that the definition of C^2 , (3.25), should include the algebraic constraints. We here confirm this using the gauge-wave evolution in Fig.6. The coefficient parameters λ_φ , λ_K , $\lambda_{\bar{\gamma}}$, $\lambda_{\bar{A}}$, and $\lambda_{\bar{\Gamma}}$ are the same as those in Fig.2. We plot each constraint equation in the panels. Panel (a) shows the case $c_G = c_A = c_S = 0$, (b) shows the case $c_G = 0, c_A = c_S = 1$, (c) shows the case $c_A = 0, c_G = c_S = 1$, and (d) shows the case $c_S = 0, c_G = c_A = 1$. In panel (a), we see that the simulation stops at $t = 800$ owing to a sudden increase in the violation of the constraint. In comparison with panel (b) in Fig.3 [$c_G = c_A = c_S = 1$], the violation of the constraint is lower if C^2 includes the algebraic constraint terms. This result is consistent with the discussion in Sec.III B. Panels (b) and (c) show that if we turn off c_G or c_A , then the violations of the \mathcal{G} -constraint or \mathcal{A} -constraint become worse than those indicated by lines (C-3) and (C-4) in Fig.3, respectively. These results are consistent with the discussion of the definition of C^2 in Sec.III B. Panel (d), on the other hand, appears similar to Fig.3. This is due to the smallness of $\lambda_{\bar{\gamma}}$ as mentioned above.

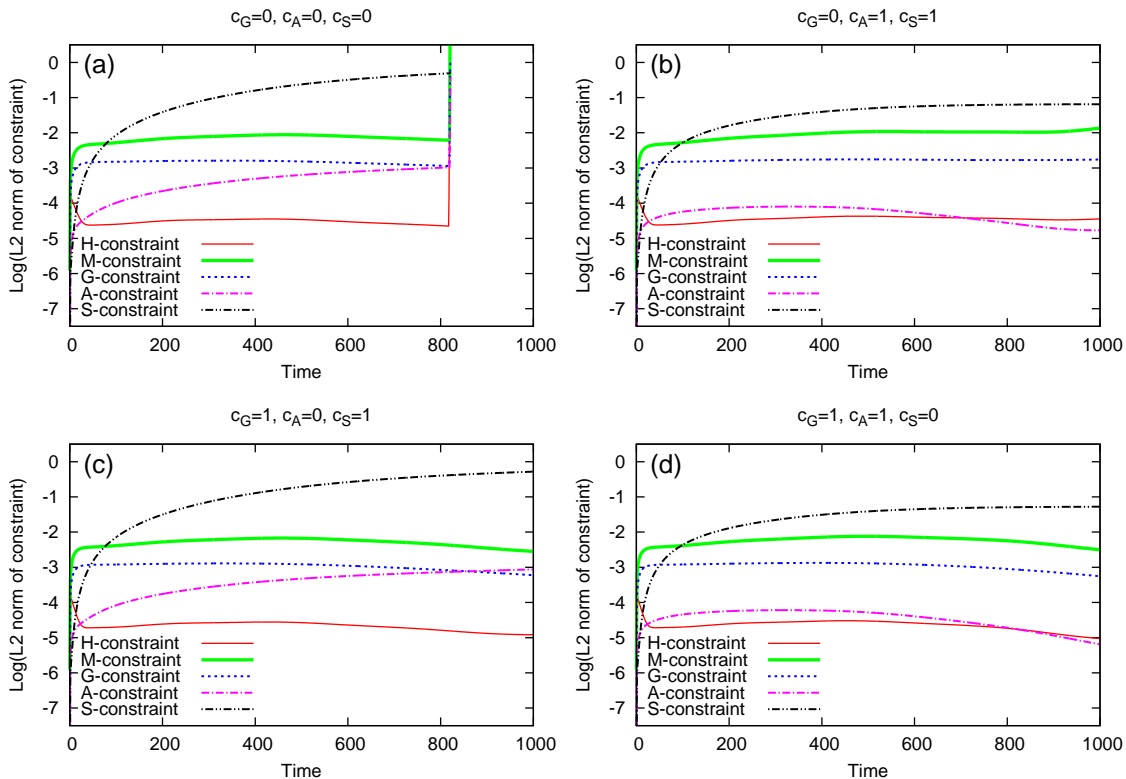


FIG. 6. Effect of differences in the definition of C^2 , (3.25), on the damping of each constraint equation. Panel (a) shows the case $c_G = c_A = c_S = 0$, (b) shows the case $c_G = 0, c_A = c_S = 1$, (c) shows the case $c_G = 1, c_A = 0, c_S = 1$, and (d) shows the case $c_G = c_A = 1, c_S = 0$. The thin solid lines are the \mathcal{H} -constraint, the thick solid lines are the \mathcal{M} -constraint, the dotted lines are the \mathcal{G} -constraint, the dot-dashed lines are the \mathcal{A} -constraint, and the two-dot-dashed lines are the \mathcal{S} -constraint.

- Simulation domain: $x \in [-0.5, 0.5], y = z = 0$.
- Grid: $x_n = -0.5 + (n - (1/2))dx$, $n = 1, \dots, 100$, where $dx = 1/100$.
- Time step: $dt = 0.25dx$.
- Boundary conditions: Periodic boundary condition in x -direction and planar symmetry in y - and z -directions.
- Gauge conditions: harmonic slicing and $\beta^i = 0$.
- Scheme: second-order iterative Crank-Nicolson.

2. Constraint Violations and Damping of Violations

We first show the case of the standard BSSN formulation, (3.6)-(3.10). Figure 7 shows the L2 norm of the violations of the constraints as a function of backward time ($-t$). We see that the violation of the \mathcal{M} -constraint is the largest at all times and that all the violations of constraints increase monotonically with time. Compared with [23], our code shows that the \mathcal{H} -constraint (A-1)

remains at the same level but the \mathcal{M} -constraint (A-2) is smaller.

Similarly to in the gauge-wave test, we compare the violations of C^2 for three types of BSSNs in Fig.8: (A) the standard BSSN formulation (3.6)-(3.10), (B) the \tilde{A} -adjusted BSSN formulation (3.6)-(3.8), (3.10), and (3.26), and (C) the C^2 -adjusted BSSN formulation (3.19)-(3.23). We adopt the parameters $\kappa_A = -10^{-0.2}$, $\lambda_\varphi = -10^{-10}$, $\lambda_K = -10^{-4.6}$, $\lambda_{\tilde{\gamma}} = -10^{-11}$, $\lambda_{\tilde{A}} = -10^{-1.2}$, and $\lambda_{\tilde{\Gamma}} = -10^{-14.3}$ to minimize the violations of the constraints at $t = -1000$ for these evolutions. In the case of the \tilde{A} -adjusted BSSN formulation, the violation of the constraints decreases if we set $|\kappa_A|$ larger than $10^{-0.2}$. In the case of the C^2 -adjusted BSSN formulation, it decreases if we set $|\lambda_{\tilde{A}}|$ larger than $10^{-1.2}$. Note that the signatures of the above κ_A and λ_S are negative, contrary to the predictions in [22] and Sec.III, respectively. This is because these simulations are performed with backward time.

As shown in Fig.8, the violations of C^2 for the standard BSSN formulation and \tilde{A} -adjusted BSSN formulation increase monotonically with time. On the other hand, that for the C^2 -adjusted BSSN formulation decreases after $t = -200$ and maintains a magnitude under $O(10^{-2})$

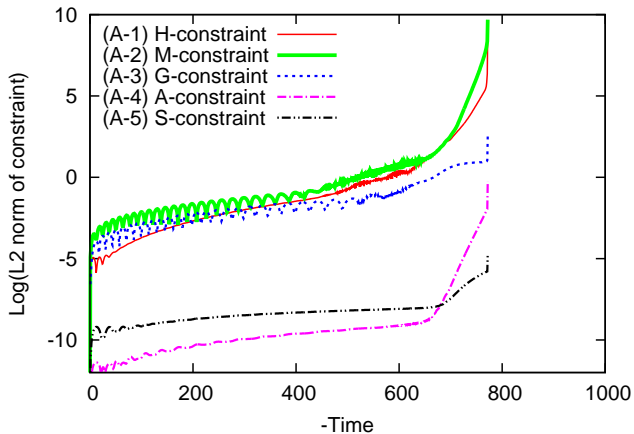


FIG. 7. L2 norm of each constraint equation in the polarized Gowdy wave evolution using the standard BSSN formulation. The vertical axis is the logarithm of the L2 norm of the constraint and the horizontal axis is backward time. The thin solid line (A-1) is the \mathcal{H} -constraint, the thick solid line (A-2) is the \mathcal{M} -constraint, the dotted line (A-3) is the \mathcal{G} -constraint, the dot-dashed line (A-4) is the \mathcal{A} -constraint, and the two-dot-dashed line (A-5) is the \mathcal{S} -constraint.

after $t = -400$.

To investigate the reason why C^2 starts to decay rapidly after $t = -200$, we plot each constraint in Fig.9. We see that the violations of the \mathcal{A} -constraint and \mathcal{S} -constraint increase with negative time, in contrast to the standard BSSN formulation, and those of the \mathcal{M} -constraint and \mathcal{G} -constraint decrease after $t = -200$. The propagation equation of the \mathcal{M} -constraint, (B2), includes the term $-2c_A \lambda_{\tilde{A}} \partial_a \mathcal{A}$, which contributes to constraint damping. Similarly, the propagation equation of the \mathcal{G} -constraint, (B3), includes $\delta^{ab} \{ (1/2) \lambda_{\tilde{\gamma}} \partial_b \Delta + 2 \lambda_{\tilde{\Gamma}} \partial_b \} \mathcal{H} - \lambda_{\tilde{\gamma}} c_S \delta^{ab} \partial_b \mathcal{S}$; the decay of the violations of the \mathcal{G} -constraint is caused by these terms. Therefore, these terms are considered to become significant of approximately $t = -200$ when the violations of the \mathcal{A} , \mathcal{H} , and \mathcal{S} -constraints become a certain order of magnitude.

In contrast to the gauge-wave testbed (Fig.4), we prepared Fig.10, which shows the magnitudes of the ratio of the L2 norm of the adjusted terms to the original terms. Since the magnitudes of the adjusted terms of φ and $\tilde{\gamma}_{ij}$ can be disregarded, the effect of the reduction of the adjusted terms of φ and $\tilde{\gamma}_{ij}$ is negligible. Therefore, the C^2 -adjusted BSSN evolution in the Gowdy wave can be regarded as maintaining its hyperbolicity.

3. Damping Effect of each Adjusted Term in C^2 -adjusted BSSN Formulation

To investigate the contribution to constraint damping of each adjusted term, (3.19)-(3.23), we perform evolutions with only one of the parameters,

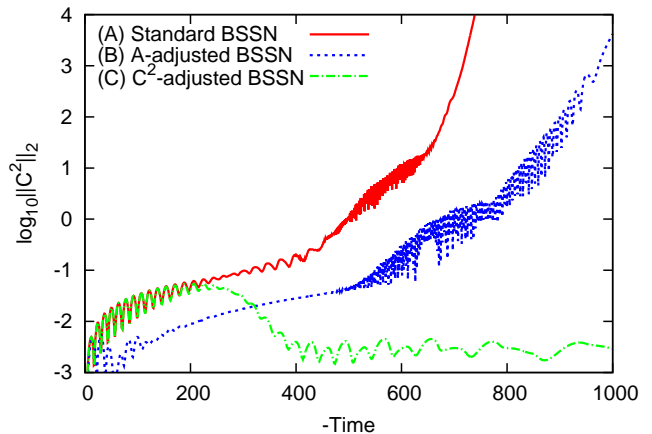


FIG. 8. L2 norm of the constraints, C^2 , of the polarized Gowdy wave tests for the standard BSSN and two adjusted formulations. The vertical axis is the logarithm of the L2 norm of C^2 and the horizontal axis is backward time. The solid line (A) is the standard BSSN formulation, the dotted line (B) is the \tilde{A} -adjusted BSSN formulation with $\kappa_A = -10^{-0.2}$, and the dot-dashed line (C) is the C^2 -adjusted BSSN formulation with $\lambda_\varphi = -10^{-10}$, $\lambda_K = -10^{-4.6}$, $\lambda_{\tilde{\gamma}} = -10^{-11}$, $\lambda_{\tilde{A}} = -10^{-1.2}$, and $\lambda_{\tilde{\Gamma}} = -10^{-14.3}$. Note that the signatures of κ_A and λ_S are negative since the simulations evolve backward. We see that lines (A) and (C) are identical until $t = -200$. Line (C) then decreases and maintains its magnitude under $O(10^{-2})$ after $t = -400$. We confirm this behavior until $t = -1500$.

($\lambda_\varphi, \lambda_K, \lambda_{\tilde{\gamma}}, \lambda_{\tilde{A}}, \lambda_{\tilde{\Gamma}}$), nonzero. Since the magnitudes of the adjusted terms of \tilde{A}_{ij} and K are largest until $t = -200$ in Fig.10, these terms are expected to be the key to reducing the constraint violation.

The effect of these terms on reducing C^2 is plotted in Fig.11. The left panel shows the case of $\lambda_{\tilde{A}} \neq 0$ with the other parameters equal to zero. The right panel shows the case of $\lambda_K \neq 0$ with the other parameters equal to zero. In the left panel, we see that the violation of C^2 decreases with increasing negative time. Therefore, the adjusted terms of \tilde{A}_{ij} contribute to the reduction of constraint violations. On the other hand, the adjusted terms of K do not appear to contribute to the reduction of constraint violations. These results are consistent with the case of the gauge-wave testbed; thus, it is important to adjust $\lambda_{\tilde{A}}$ to an appropriate value to control the constraints.

4. Damping Effect of Algebraic Constraints

In Sec.III, we investigated the effect of the definition of C^2 . Similarly to the gauge-wave test in the previous subsection, we here show the effect of constraint damping caused by the algebraic constraints. The coefficient parameters, $\lambda_\varphi, \lambda_K, \lambda_{\tilde{\gamma}}, \lambda_{\tilde{A}}$ and $\lambda_{\tilde{\Gamma}}$, are all the same as

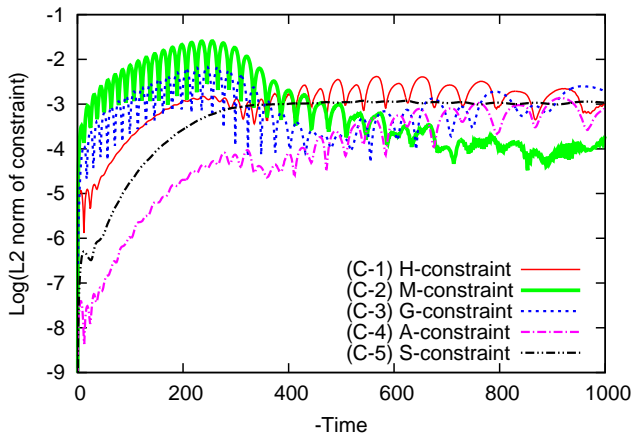


FIG. 9. As Fig.7 but for the C^2 -adjusted BSSN formulation. The parameters, $(\lambda_\varphi, \lambda_K, \lambda_{\tilde{\gamma}}, \lambda_{\tilde{A}}, \lambda_{\tilde{\Gamma}})$, are all the same as those for (C) in Fig.8. We see that the violation of the \mathcal{M} -constraint decreases and becomes the lowest after $t = -700$.

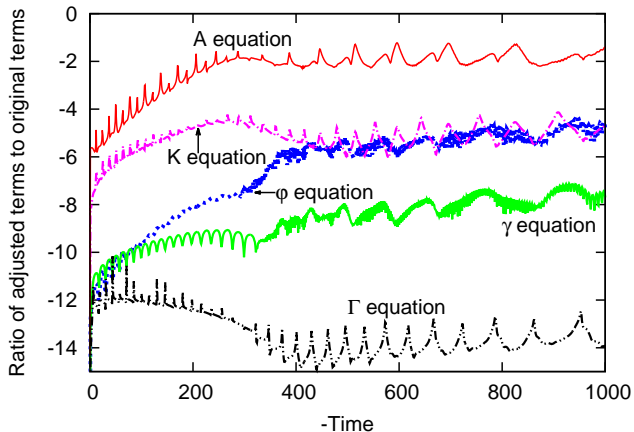


FIG. 10. L2 norm of (additional terms)/(original terms) of each evolution equation for the C^2 -adjusted BSSN formulation, (3.19)-(3.23). We see that the largest ratio is that for the evolution of \tilde{A}_{ij} . The corrections to the $\tilde{\gamma}_{ij}$ and $\tilde{\Gamma}^i$ evolution equations are reasonably small.

those for (C) in Fig.8.

In Figs.12 (a) and (c), we see that all the violations of the constraints are larger than those in Fig.9. These results are consistent with the discussion in Sec.III B. On the other hand, the violations of each constraint in panels (b) and (d) almost overlap with those in Fig.9. These results are, however, not contradictory. For example, the parameter c_G appears in the terms $c_G(-1/2)\lambda_{\tilde{\gamma}}\Delta\partial_m - 2\lambda_{\tilde{\Gamma}}\partial_m)\mathcal{G}^m$ in (B1), $c_G(\lambda_{\tilde{\gamma}}\Delta - 2\lambda_{\tilde{\Gamma}})\mathcal{G}^a$ in (B3), and $c_G\lambda_{\tilde{\gamma}}\partial_\ell\mathcal{G}^\ell$ in (B5). All these terms include $\lambda_{\tilde{\gamma}}$ or $\lambda_{\tilde{\Gamma}}$. Both $\lambda_{\tilde{\gamma}}$ and $\lambda_{\tilde{\Gamma}}$ are set to reasonably small values in these simulations; thus, a reduction of the constraint violations owing to the existence of the \mathcal{G} -constraint in

C^2 is not observable. Therefore, a difference in the violations of the constraints between panel (b) and Fig.9 is not distinguishable. Similarly, the parameter c_S appears in the terms $3c_S\lambda_{\tilde{\gamma}}\Delta\mathcal{S}$ in (B1), $-c_S\lambda_{\tilde{\gamma}}\delta^{ab}\partial_b\mathcal{S}$ in (B3), and $-6\lambda_{\tilde{\gamma}}c_S\mathcal{S}$ in (B5), all of which include $\lambda_{\tilde{\gamma}}$. Consequently, the constraint-damping effect via the algebraic constraints \mathcal{G} , \mathcal{A} , and \mathcal{S} is apparent.

V. SUMMARY AND DISCUSSION

To obtain an evolution system robust against the violation of constraints, we derived a new set of adjusted BSSN equations applying the idea proposed by Fiske [24] to obtain what we call a “ C^2 -adjusted system.”

That is, we added the functional derivatives of the norm of the constraints, C^2 , to the evolution equations [(3.19)-(3.23)]. This implementation was applied to the ADM formulation in our previous study [26] and is applied to the BSSN equations in this study. We performed numerical tests in the gauge-wave and Gowdy wave testbeds and confirmed that the violations of constraints decrease as expected, and that longer and accurate simulation than that for the standard BSSN evolution is possible.

The construction of the C^2 -adjusted system is straightforward. However, in BSSN, there are two kinetic constraints and three algebraic constraints; thus, the definition of C^2 is a matter of concern. By analyzing constraint propagation equations, we concluded that C^2 should include all the constraints. This was also confirmed by numerical tests.

To evaluate the reduction of the violations of the constraints for the C^2 -adjusted BSSN formulation, we also performed evolutions for the \tilde{A} -adjusted BSSN formulation proposed in [22]. We concluded that the C^2 -adjusted BSSN formulation exhibits superior constraint damping to the standard and \tilde{A} -adjusted BSSN formulations. In particular, the lifetimes of the simulations for the C^2 -adjusted BSSN formulation in the gauge-wave and Gowdy wave testbeds were ten times and two times larger than those for the standard BSSN formulation, respectively.

Fiske reported the applications of the idea of C^2 -adjustment to “linearized” ADM and BSSN formulations in his dissertation [25]. (As he mentioned, his BSSN is not derived from the standard BSSN equations but from a linearized ADM using a new variable, Γ . His set of BSSN equations also does not include the \mathcal{A} - and \mathcal{S} -constraints in our notation.). He observed damping of the constraint violation of five orders of magnitude and the equivalent solution errors in his numerical evolution tests. Our studies reported in this article show that the full BSSN set of equations with fully adjusted terms also produces the desired constraint-damping results (Fig.2 and Fig.8); although improvements of fewer orders of magnitude were obtained, the improvements are apparent.

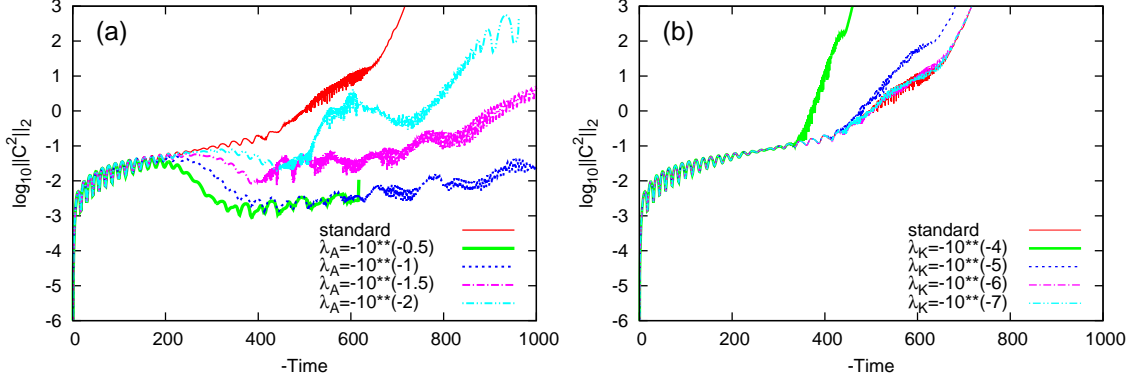


FIG. 11. Effect of adjusting parameters for the C^2 -adjusted BSSN formulations, (3.19)-(3.21). The left panel shows the case when $\lambda_{\tilde{A}} \neq 0$ and the other parameters are zero. We see that the value $\lambda_{\tilde{A}} = -10^{-1}$ exhibits the best performance for controlling C^2 . (The standard BSSN case diverges at $t = -750$, while the case $\lambda_{\tilde{A}} = -10^{-1}$ diverges at $t = -1500$.) The right panel shows the case when $\lambda_K \neq 0$ and the other parameters are zero. However, the violation of C^2 is larger than that for the standard BSSN formulation if only λ_K is used for adjustment with the other parameters equal to zero.

We found in the application to the ADM system [26] that the adjustment to the K_{ij} -evolution equation is essential. In the present study, we found that the adjustment to the \tilde{A}_{ij} -evolution equation is essential for controlling the constraints. In both cases, the associated adjustment parameters (Lagrangian multipliers), $\lambda_{\tilde{A}}$ in this study, are reasonably sensitive and require fine-tuning. Methods of monitoring the order of constraint violations and maintaining them by tuning the parameters automatically would be useful. Applications of control theory in this direction are being investigated.

The correction terms of the C^2 -adjusted system include higher-order derivatives and are not quasi-linear; thus, little is known mathematically about such systems. These additional terms might effectively act as artificial viscosity terms in fluid simulations, but might also enhance the violation of errors. To investigate this direction further, the next step is to apply the idea to a system in

which constraints do not include second-order derivatives of dynamical variables. We are working on the Kidder-Scheel-Teukolsky formulation [10] as an example of such a system, which we hope to report in the near future.

ACKNOWLEDGMENTS

This work was partially supported by Grant-in-Aid for Scientific Research Fund of Japan Society of the Promotion of Science No. 22540293 (HS). Numerical computations were carried out on an Altix 3700 BX2 supercomputer at YITP in Kyoto University and on the RIKEN Integrated Cluster of Clusters (RICC).

Appendix A: Additional C^2 -adjusted terms

The adjusted terms $\delta C^2/\delta\varphi$, $\delta C^2/\delta K$, $\delta C^2/\delta\tilde{\gamma}_{mn}$, $\delta C^2/\delta\tilde{A}_{mn}$, and $\delta C^2/\delta\tilde{\Gamma}^a$ in (3.19)-(3.23) are written as follows:

$$\begin{aligned} \frac{\delta C^2}{\delta\varphi} = & 2\bar{H}_1\mathcal{H} - 2(\partial_a\bar{H}_2^a)\mathcal{H} - 2\bar{H}_2^a\partial_a\mathcal{H} + 2(\partial_a\partial_b\bar{H}_3^{ab})\mathcal{H} + 2(\partial_a\bar{H}_3^{ab})\partial_b\mathcal{H} + 2(\partial_b\bar{H}_3^{ab})\partial_a\mathcal{H} + 2\bar{H}_3^{ab}\partial_a\partial_b\mathcal{H} \\ & - 2(\partial_a\bar{M}_{1i}^a)e^{-4\varphi}\tilde{\gamma}^{ij}\mathcal{M}_j + 8\bar{M}_{1i}^ae^{-4\varphi}(\partial_a\varphi)\tilde{\gamma}^{ij}\mathcal{M}_j - 2\bar{M}_{1i}^ae^{-4\varphi}(\partial_a\tilde{\gamma}^{ij})\mathcal{M}_j - 2\bar{M}_{1i}^ae^{-4\varphi}\tilde{\gamma}^{ij}\partial_a\mathcal{M}_j \\ & - 4\tilde{\gamma}^{ij}e^{-4\varphi}\mathcal{M}_i\mathcal{M}_j + 4c_Ge^{4\varphi}\tilde{\gamma}_{ij}\mathcal{G}^i\mathcal{G}^j, \end{aligned} \quad (\text{A1})$$

$$\frac{\delta C^2}{\delta K} = 2\bar{H}_4\mathcal{H} - 2(\partial_\ell\bar{M}_{2i}^\ell)e^{-4\varphi}\tilde{\gamma}^{ij}\mathcal{M}_j + 8\bar{M}_{2i}^\ell e^{-4\varphi}(\partial_\ell\varphi)\tilde{\gamma}^{ij}\mathcal{M}_j - 2\bar{M}_{2i}^\ell e^{-4\varphi}(\partial_\ell\tilde{\gamma}^{ij})\mathcal{M}_j - 2\bar{M}_{2i}^\ell e^{-4\varphi}\tilde{\gamma}^{ij}\partial_\ell\mathcal{M}_j, \quad (\text{A2})$$

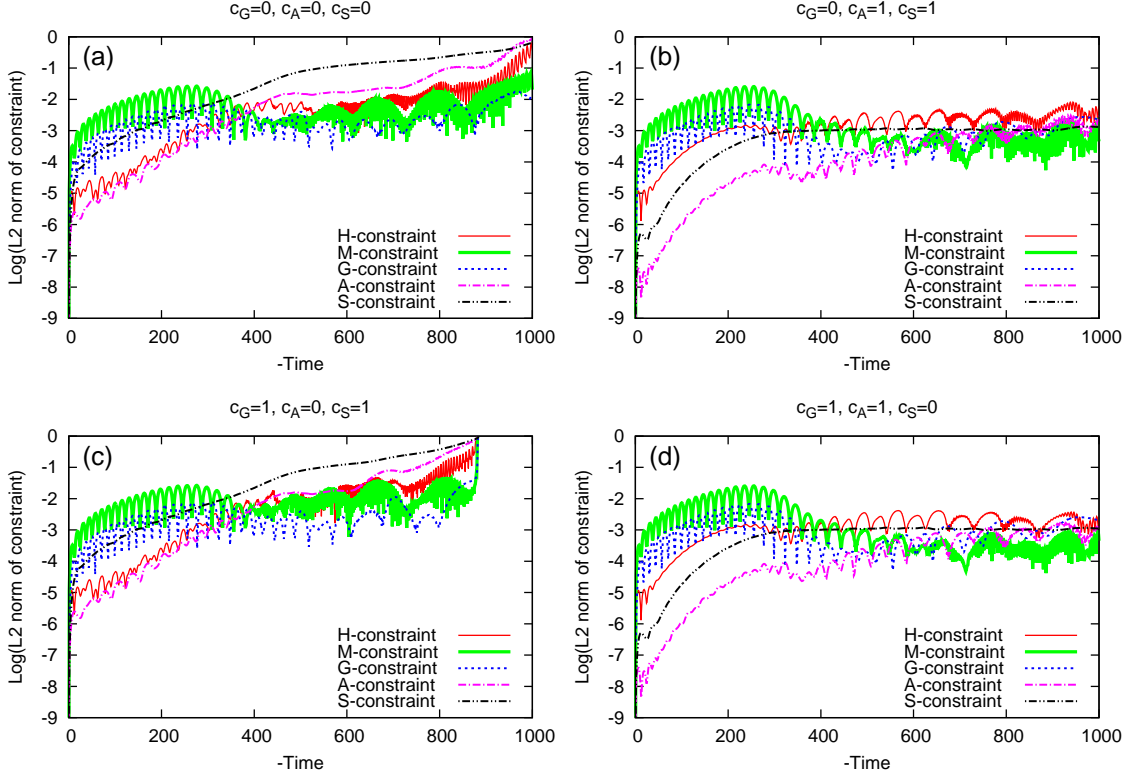


FIG. 12. Effect of differences in the definition of C^2 . Panel (a) shows the case $c_G = c_A = c_S = 0$, panel (b) shows the case $c_G = 0, c_A = c_S = 1$, panel (c) shows the case $c_G = 1, c_A = 0$, and $c_S = 1$, and panel (d) shows the case $c_G = c_A = 1$ and $c_S = 0$. In comparison with Fig.9, all the violations of the constraints in (a) and (c) are larger. On the other hand, the lines in (b) and (d) are almost identical.

$$\begin{aligned}
\frac{\delta C^2}{\delta \tilde{\gamma}_{mn}} &= 2\bar{H}_5^{mn}\mathcal{H} - 2(\partial_i \bar{H}_6^{imn})\mathcal{H} - 2\bar{H}_6^{imn}\partial_i\mathcal{H} + 2(\partial_i \partial_j \bar{H}_7^{ijmn})\mathcal{H} + 2(\partial_i \bar{H}_7^{ijmn})\partial_j\mathcal{H} + 2(\partial_j \bar{H}_7^{ijmn})\partial_i\mathcal{H} \\
&\quad + 2\bar{H}_7^{ijmn}\partial_i\partial_j\mathcal{H} + 2\bar{M}_{3i}{}^{mn}e^{-4\varphi}\tilde{\gamma}^{ij}\mathcal{M}_j - 2(\partial_c \bar{M}_{4i}{}^{cmn})e^{-4\varphi}\tilde{\gamma}^{ij}\mathcal{M}_j + 8\bar{M}_{4i}{}^{cmn}e^{-4\varphi}(\partial_c\varphi)\tilde{\gamma}^{ij}\mathcal{M}_j \\
&\quad - 2\bar{M}_{4i}{}^{cmn}e^{-4\varphi}(\partial_c\tilde{\gamma}^{ij})\mathcal{M}_j - 2\bar{M}_{4i}{}^{cmn}e^{-4\varphi}\tilde{\gamma}^{ij}\partial_c\mathcal{M}_j - e^{-4\varphi}\tilde{\gamma}^{im}\tilde{\gamma}^{jn}\mathcal{M}_i\mathcal{M}_j + 2c_G G_1^{imn}e^{4\varphi}\tilde{\gamma}_{ij}\mathcal{G}^j \\
&\quad - 2c_G(\partial_\ell G_2^{imnl})e^{4\varphi}\tilde{\gamma}_{ij}\mathcal{G}^j - 8c_G G_2^{imnl}e^{4\varphi}(\partial_\ell\varphi)\tilde{\gamma}_{ij}\mathcal{G}^j - 2c_G G_2^{imnl}e^{4\varphi}(\partial_\ell\tilde{\gamma}_{ij})\mathcal{G}^j - 2c_G G_2^{imnl}e^{4\varphi}\tilde{\gamma}_{ij}\partial_\ell\mathcal{G}^j \\
&\quad + c_G e^{4\varphi}G^m\mathcal{G}^n + 2c_A A_1^{mn}\mathcal{A} + 2c_S S_1^{mn}\mathcal{S}, \tag{A3}
\end{aligned}$$

$$\begin{aligned}
\frac{\delta C^2}{\delta \tilde{A}_{mn}} &= 2\bar{H}_8^{mn}\mathcal{H} + 2e^{-4\varphi}\tilde{\gamma}^{ij}\bar{M}_{5i}{}^{mn}\mathcal{M}_j - 2(\partial_c \bar{M}_{6i}{}^{cmn})e^{-4\varphi}\tilde{\gamma}^{ij}\mathcal{M}_j + 8\bar{M}_{6i}{}^{cmn}e^{-4\varphi}(\partial_c\varphi)\tilde{\gamma}^{ij}\mathcal{M}_j \\
&\quad - 2\bar{M}_{6i}{}^{cmn}e^{-4\varphi}(\partial_c\tilde{\gamma}^{ij})\mathcal{M}_j - 2\bar{M}_{6i}{}^{cmn}e^{-4\varphi}\tilde{\gamma}^{ij}\partial_c\mathcal{M}_j + 2c_A A_2^{mn}\mathcal{A}, \tag{A4}
\end{aligned}$$

$$\frac{\delta C^2}{\delta \tilde{\Gamma}^a} = 2\bar{H}_{9a}\mathcal{H} - 2(\partial_b \bar{H}_{10a}^b)\mathcal{H} - 2\bar{H}_{10a}^b\partial_b\mathcal{H} + 2c_G G_{3a}^i e^{4\varphi}\tilde{\gamma}_{ij}\mathcal{G}^j, \tag{A5}$$

where

$$\bar{H}_1 = -4e^{-4\varphi}\tilde{R} + 32e^{-4\varphi}\{\tilde{D}^i\tilde{D}_i\varphi + (\tilde{D}_i\varphi)(\tilde{D}^i\varphi)\}, \tag{A6}$$

$$\bar{H}_2^a = 8e^{-4\varphi}(\tilde{\gamma}^{ij}\tilde{\Gamma}_{ij}^a - 2\tilde{D}^a\varphi), \tag{A7}$$

$$\bar{H}_3^{ab} = -8e^{-4\varphi}\tilde{\gamma}^{ab}, \tag{A8}$$

$$\bar{H}_4 = (4/3)K - (2/3)\tilde{\gamma}^{ij}\tilde{A}_{ij}, \tag{A9}$$

$$\begin{aligned}
\bar{H}_5^{mn} &= -e^{-4\varphi}\tilde{R}^{mn} + e^{-4\varphi}(\partial_j\tilde{\Gamma}^{(m}\tilde{\gamma}^{n)j}) \\
&\quad - 2e^{-4\varphi}\tilde{\Gamma}^{km}{}_j\tilde{\Gamma}^{jn}{}_k - 2e^{-4\varphi}\tilde{\Gamma}^{il(m}\tilde{\Gamma}^{n)}{}_{\ell i} \\
&\quad - e^{-4\varphi}\tilde{\Gamma}^{ami}\tilde{\Gamma}{}_{ai}{}^n - e^{-4\varphi}\tilde{\Gamma}^{mil}\tilde{\Gamma}{}_{li}{}^n \\
&\quad + (1/2)e^{-4\varphi}\tilde{\gamma}_{ij,al}\tilde{\gamma}^{ij}\tilde{\gamma}^{am}\tilde{\gamma}^{\ell n} + 8e^{-4\varphi}\tilde{D}^m\tilde{D}^n\varphi \\
&\quad - 8e^{-4\varphi}(\tilde{D}^{(m}\varphi)\tilde{\Gamma}^{n)}{}_{ij}\tilde{\gamma}^{ij} + 8e^{-4\varphi}(\tilde{D}^m\varphi)(\tilde{D}^n\varphi) \\
&\quad + 2\tilde{A}^{mb}\tilde{A}{}^n{}_b + (2/3)\tilde{A}^{mn}K, \tag{A10}
\end{aligned}$$

$$\begin{aligned}
\bar{H}_6^{\ell mn} &= e^{-4\varphi}\{\tilde{\Gamma}^{\ell mn} + 2\tilde{\Gamma}^{(nm)\ell} + (1/2)\Gamma^\ell\tilde{\gamma}^{mn} \\
&\quad + 8\tilde{\gamma}^{\ell(m}\tilde{D}^{n)}\varphi - 4\tilde{\gamma}^{mn}\tilde{D}^\ell\varphi\}, \tag{A11}
\end{aligned}$$

$$\bar{H}_7^{ijmn} = -(1/2)e^{-4\varphi}\tilde{\gamma}^{mn}\tilde{\gamma}^{ij}, \tag{A12}$$

$$\bar{H}_8^{mn} = -2\tilde{A}^{mn} - (2/3)\tilde{\gamma}^{mn}K, \tag{A13}$$

$$\bar{H}_{9a} = (1/2)e^{-4\varphi}\tilde{\gamma}^{ij}\tilde{\gamma}_{ij,a}, \tag{A14}$$

$$\bar{H}_{10a}^b = e^{-4\varphi}\delta^b{}_a, \tag{A15}$$

$$\bar{M}_{1i}{}^a = 6\tilde{A}{}^a{}_i - 2\tilde{A}_{mn}\tilde{\gamma}^{mn}\delta^a{}_i, \tag{A16}$$

$$\bar{M}_{2i}{}^j = -(2/3)\delta^j{}_i, \tag{A17}$$

$$\begin{aligned}
\bar{M}_{3i}{}^{mn} &= -6(\tilde{D}^{(m}\varphi)\tilde{A}{}^n)_{i} + 2(\tilde{D}_i\varphi)\tilde{A}^{mn} - \tilde{D}^{(m}\tilde{A}{}^n)_{i} \\
&\quad + \tilde{A}^{a(n}\tilde{\Gamma}^m)_{ai} + \tilde{A}_i{}^{(m}\tilde{\Gamma}^{n)}{}_{j\ell}\tilde{\gamma}^{j\ell}, \tag{A18}
\end{aligned}$$

$$\bar{M}_{4i}{}^{cmn} = -\tilde{\gamma}^{c(n}\tilde{A}{}^m)_{i} + (1/2)\tilde{\gamma}^{mn}\tilde{A}{}^c{}_i - (1/2)\tilde{A}^{nm}\delta^c{}_i, \tag{A19}$$

$$\begin{aligned}
\bar{M}_{5i}{}^{mn} &= 6(\tilde{D}^{(m}\varphi)\delta^n)_{i} - 2(\tilde{D}_i\varphi)\tilde{\gamma}^{mn} - \delta_i{}^{(m}\tilde{\Gamma}^{n)}{}_{j\ell}\tilde{\gamma}^{j\ell} \\
&\quad + (1/2)\tilde{\gamma}^{mn}{}_{,i}, \tag{A20}
\end{aligned}$$

$$\bar{M}_{6i}{}^{cmn} = \tilde{\gamma}^{c(m}\delta^n)_{i}, \tag{A21}$$

$$G_1^{iab} = \tilde{\Gamma}^{iab} + \tilde{\gamma}^{i(b}\tilde{\Gamma}^{a)}{}_{mn}\tilde{\gamma}^{mn}, \tag{A22}$$

$$G_2^{iabl} = -\tilde{\gamma}^{\ell(b}\tilde{\gamma}^{a)l} + (1/2)\tilde{\gamma}^{ab}\tilde{\gamma}^{i\ell}, \tag{A23}$$

$$G_{3j}^i = \delta^i{}_j, \tag{A24}$$

$$A_1^{ab} = -\tilde{A}^{ab}, \tag{A25}$$

$$A_2^{ab} = \tilde{\gamma}^{ab}, \tag{A26}$$

$$S_1^{ab} = (1/2)\varepsilon^{ajk}\varepsilon^{bn\ell}. \tag{A27}$$

Appendix B: Constraint Propagation Equations for C^2 -adjusted BSSN Formulation and \tilde{A} -adjusted BSSN Formulation in Minkowskii spacetime

Here we give the constraint propagation equations for the C^2 -adjusted BSSN formulation and \tilde{A} -adjusted BSSN formulation in Minkowskii spacetime. For simplicity, we set $\lambda_{\tilde{\gamma}ijmn} = \lambda_{\tilde{\gamma}}\delta_{im}\delta_{jn}$, $\lambda_{\tilde{A}ijmn} = \lambda_{\tilde{A}}\delta_{im}\delta_{jn}$, and $\lambda_{\tilde{\Gamma}}^{ij} = \lambda_{\tilde{\Gamma}}\delta^{ij}$. The constraint propagation equations for the C^2 -adjusted BSSN formulation are

$$\partial_t\mathcal{H} = [\text{Original Terms}] + (-128\lambda_\varphi\Delta^2 - (3/2)\lambda_{\tilde{\gamma}}\Delta^2 + 2\lambda_{\tilde{\Gamma}}\Delta)\mathcal{H} + c_G(-1/2)\lambda_{\tilde{\gamma}}\Delta\partial_m - 2\lambda_{\tilde{\Gamma}}\partial_m)\mathcal{G}^m + 3c_S\lambda_{\tilde{\gamma}}\Delta\mathcal{S}, \tag{B1}$$

$$\partial_t\mathcal{M}_a = [\text{Original Terms}] + \left\{ (8/9)\lambda_K\delta^{bc}\partial_a\partial_b + \lambda_{\tilde{A}}\Delta\delta_a{}^c + \lambda_{\tilde{A}}\delta^{bc}\partial_a\partial_b \right\}\mathcal{M}_c - 2c_A\lambda_{\tilde{A}}\partial_a\mathcal{A}, \tag{B2}$$

$$\partial_t\mathcal{G}^a = [\text{Original Terms}] + \delta^{ab}\left((1/2)\lambda_{\tilde{\gamma}}\partial_b\Delta + 2\lambda_{\tilde{\Gamma}}\partial_b\right)\mathcal{H} + c_G(\lambda_{\tilde{\gamma}}\Delta\delta^a{}_b + (1/2)\lambda_{\tilde{\gamma}}\delta^{ac}\partial_c\partial_b - 2\lambda_{\tilde{\Gamma}}\delta^a{}_b)\mathcal{G}^b - \lambda_{\tilde{\gamma}}c_S\delta^{ab}\partial_b\mathcal{S}, \tag{B3}$$

$$\partial_t\mathcal{A} = [\text{Original Terms}] + 2\lambda_{\tilde{A}}\delta^{ij}(\partial_i\mathcal{M}_j) - 6c_A\lambda_{\tilde{A}}\mathcal{A}, \tag{B4}$$

$$\partial_t\mathcal{S} = [\text{Original Terms}] + 3\lambda_{\tilde{\gamma}}\Delta\mathcal{H} + c_G\lambda_{\tilde{\gamma}}\partial_\ell\mathcal{G}^\ell - 6c_S\lambda_{\tilde{\gamma}}\mathcal{S}, \tag{B5}$$

and those of the \tilde{A} -adjusted BSSN formulation are

$$\partial_t\mathcal{H} = [\text{Original Terms}], \tag{B6}$$

$$\partial_t\mathcal{M}_i = [\text{Original Terms}] + (1/2)\kappa_A\Delta\mathcal{M}_i, \tag{B7}$$

$$\partial_t\mathcal{G}^i = [\text{Original Terms}], \tag{B8}$$

$$\partial_t\mathcal{A} = [\text{Original Terms}] + \kappa_A\delta^{ij}\partial_i\mathcal{M}_j, \tag{B9}$$

$$\partial_t\mathcal{S} = [\text{Original Terms}], \tag{B10}$$

where Δ is the Laplacian operator in flat space. ‘‘Original Terms’’ refers to the right-hand side of the constraint propagation equations for the standard BSSN formulation. Full expressions for the terms are given in the ap-

pendix of [22].

expressions are available in the appendix of [22]).

Appendix C: Constraint Propagation Equations for BSSN Formulation with $\beta^i = 0$

The constraint propagation equations for the standard BSSN formulation with $\beta^i = 0$ are as follows (the full

$$\begin{aligned}
\partial_t \mathcal{H} = & [(2/3)\alpha K + (2/3)\alpha \mathcal{A}] \mathcal{H} + [-4e^{-4\varphi} \alpha (\alpha_k \varphi) \tilde{\gamma}^{kj} - 2e^{-4\varphi} (\partial_k \alpha) \tilde{\gamma}^{jk}] \mathcal{M}_j \\
& + [-2\alpha e^{-4\varphi} \tilde{A}^k_j \partial_k - \alpha e^{-4\varphi} (\partial_j \tilde{A}_{k\ell}) \tilde{\gamma}^{k\ell} - e^{-4\varphi} (\partial_j \alpha) \mathcal{A}] \mathcal{G}^j \\
& + [2\alpha e^{-4\varphi} \tilde{\gamma}^{-1} \tilde{\gamma}^{\ell k} (\partial_\ell \varphi) \mathcal{A} \partial_k + (1/2)\alpha e^{-4\varphi} \tilde{\gamma}^{-1} (\partial_\ell \mathcal{A}) \tilde{\gamma}^{\ell k} \partial_k + (1/2)e^{-4\varphi} \tilde{\gamma}^{-1} (\partial_\ell \alpha) \tilde{\gamma}^{\ell k} \mathcal{A} \partial_k] \mathcal{S} \\
& + [(4/9)\alpha K \mathcal{A} - (8/9)\alpha K^2 + (4/3)\alpha e^{-4\varphi} (\partial_i \partial_j \varphi) \tilde{\gamma}^{ij} + (8/3)\alpha e^{-4\varphi} (\partial_k \varphi) (\partial_\ell \tilde{\gamma}^{\ell k}) + \alpha e^{-4\varphi} (\partial_j \tilde{\gamma}^{jk}) \partial_k \\
& + 8\alpha e^{-4\varphi} \tilde{\gamma}^{jk} (\partial_j \varphi) \partial_k + \alpha e^{-4\varphi} \tilde{\gamma}^{jk} \partial_j \partial_k + 8e^{-4\varphi} (\partial_\ell \alpha) (\partial_k \varphi) \tilde{\gamma}^{\ell k} + e^{-4\varphi} (\partial_\ell \alpha) (\partial_k \tilde{\gamma}^{\ell k}) + 2e^{-4\varphi} (\partial_\ell \alpha) \tilde{\gamma}^{\ell k} \partial_k \\
& + e^{-4\varphi} \tilde{\gamma}^{\ell k} (\partial_\ell \partial_k \alpha)] \mathcal{A}, \tag{C1}
\end{aligned}$$

$$\begin{aligned}
\partial_t \mathcal{M}_i = & [-(1/3)(\partial_i \alpha) + (1/6)\partial_i] \mathcal{H} + \alpha K \mathcal{M}_i + [\alpha e^{-4\varphi} \tilde{\gamma}^{km} (\partial_k \varphi) (\partial_j \tilde{\gamma}_{mi}) - (1/2)\alpha e^{-4\varphi} \tilde{\Gamma}^m_{k\ell} \tilde{\gamma}^{k\ell} (\partial_j \tilde{\gamma}_{mi}) \\
& + (1/2)\alpha e^{-4\varphi} \tilde{\gamma}^{mk} (\partial_k \partial_j \tilde{\gamma}_{mi}) + (1/2)\alpha e^{-4\varphi} \tilde{\gamma}^{-2} (\partial_i \mathcal{S}) (\partial_j \mathcal{S}) - (1/4)\alpha e^{-4\varphi} (\partial_i \tilde{\gamma}_{k\ell}) (\partial_j \tilde{\gamma}^{k\ell}) \\
& + \alpha e^{-4\varphi} \tilde{\gamma}^{km} (\partial_k \varphi) \tilde{\gamma}_{ji} \partial_m + \alpha e^{-4\varphi} (\partial_j \varphi) \partial_i - (1/2)\alpha e^{-4\varphi} \tilde{\Gamma}^m_{k\ell} \tilde{\gamma}^{k\ell} \tilde{\gamma}_{ji} \partial_m + \alpha e^{-4\varphi} \tilde{\gamma}^{mk} \tilde{\Gamma}_{ijk} \partial_m \\
& + (1/2)\alpha e^{-4\varphi} \tilde{\gamma}^{\ell k} \tilde{\gamma}_{ji} \partial_k \partial_\ell + (1/2)e^{-4\varphi} \tilde{\gamma}^{mk} (\partial_j \tilde{\gamma}_{im}) (\partial_k \alpha) + (1/2)e^{-4\varphi} (\partial_j \alpha) \partial_i + (1/2)e^{-4\varphi} \tilde{\gamma}^{mk} \tilde{\gamma}_{ji} (\partial_k \alpha) \partial_m] \mathcal{G}^j \\
& + [-\tilde{A}^k_i (\partial_k \alpha) + (1/9)(\alpha_j) K + (4/9)\alpha (\partial_i K) + (1/9)\alpha K \partial_i - \alpha \tilde{A}^k_i \partial_k] \mathcal{A}, \tag{C2}
\end{aligned}$$

$$\partial_t \mathcal{G}^i = 2\alpha \tilde{\gamma}^{ij} \mathcal{M}_j + [4\alpha \tilde{\gamma}^{ij} (\tilde{D}_j \varphi) - \alpha \tilde{\gamma}^{ij} \partial_j - (\partial_k \alpha) \tilde{\gamma}^{ik}] \mathcal{A}, \tag{C3}$$

$$\partial_t \mathcal{A} = \alpha K \mathcal{A}, \tag{C4}$$

$$\partial_t \mathcal{S} = -2\alpha \tilde{\gamma} \mathcal{A}. \tag{C5}$$

-
- | | |
|--------------------------------------------------------------------------------------------------------------------------------------------------------------------------------------------------------------------------------------------------------------------------------------------------------------------------------------------------------------------------------------------------------------------------------------------------------------------------------------------------------------------------------------------------------------------------------------------------------------------------------------------------------------------------------------------------------------------------------------------------------------------------------------------------------------------------------------------------------------------------------------------------------------------------------------------------------------------------------------------------------------------------------------------------------------------------------------------------------------------------------------------------------------------------------------------------|-------------------------------------------------------------------------------------------------------------------------------------------------------------------------------------------------------------------------------------------------------------------------------------------------------------------------------------------------------------------------------------------------------------------------------------------------------------------------------------------------------------------------------------------------------------------------------------------------------------------------------------------------------------------------------------------------------------------------------------------------------------------------------------------------------------------------------------------------------------------------------------------------------------------------------------------------------------------------------------------------------------------------------------------------------------------------------------------------------------|
| <p>[1] R. Arnowitt, S. Deser, and C. W. Misner, in <i>Gravitation: An Introduction to Current Research</i>, edited by L. Witten (Wiley, New York, 1962).</p> <p>[2] J. W. York, Jr., in <i>Sources of Gravitational Radiation</i>, edited by L. Smarr (Cambridge, 1979); L. Smarr and J. W. York, Jr., Phys. Rev. D 17, 2529 (1978).</p> <p>[3] H. Shinkai and G. Yoneda, Classical Quantum Gravity 17, 4799 (2000).</p> <p>[4] H. Shinkai and G. Yoneda, gr-qc/0209111 (2002).</p> <p>[5] H. Shinkai, J. Korean Phys. Soc. 54, 2513 (2009).</p> <p>[6] M. Shibata and T. Nakamura, Phys. Rev. D 52, 5428 (1995).</p> <p>[7] T. W. Baumgarte and S. L. Shapiro, Phys. Rev. D 59, 024007 (1998).</p> <p>[8] F. Pretorius, Classical Quantum Gravity 22, 425 (2005).</p> <p>[9] D. Garfinkle, Phys. Rev. D 65, 044029 (2002).</p> <p>[10] L. E. Kidder, M. A. Scheel, and S. A. Teukolsky, Phys. Rev. D 64, 064017 (2001).</p> <p>[11] C. Bona, T. Ledvinka, C. Palenzuela, and M. Žáček, Phys. Rev. D 67, 104005 (2003).</p> <p>[12] C. Bona, T. Ledvinka, C. Palenzuela, and M. Žáček, Phys. Rev. D 69, 064036 (2004).</p> | <p>[13] M. Campanelli, C. O. Lousto, P. Marronetti, and Y. Zlochower, Phys. Rev. Lett. 96, 111101 (2006).</p> <p>[14] J. G. Baker, J. Centrella, D.-I. Choi, M. Koppitz, and J. van Meter, Phys. Rev. Lett. 96, 111102 (2006).</p> <p>[15] F. Pretorius, Phys. Rev. Lett. 95, 121101 (2005).</p> <p>[16] M. A. Scheel, M. Boyle, T. Chu, L. E. Kidder, K. D. Matthews, and H. P. Pfeiffer, Phys. Rev. D 79, 024003 (2009).</p> <p>[17] D. Alic, C. Bona-Casas, C. Bona, L. Rezzolla, and C. Palenzuela, gr-qc/1106.2254 (2011).</p> <p>[18] C. Gundlach, G. Calabrese, I. Hinder, and J. M. Martín-García, Classical Quantum Gravity 22, 3767 (2005).</p> <p>[19] A. Weyhausen, S. Bernuzzi, and D. Hilditch, gr-qc/1107.5539 (2011).</p> <p>[20] G. Yoneda and H. Shinkai, Phys. Rev. D 63, 124019 (2001).</p> <p>[21] H. Shinkai and G. Yoneda, Classical Quantum Gravity 19, 1027 (2002).</p> <p>[22] G. Yoneda and H. Shinkai, Phys. Rev. D 66, 124003 (2002).</p> <p>[23] K. Kiuchi and H. Shinkai, Phys. Rev. D 77, 044010 (2008).</p> |
|--------------------------------------------------------------------------------------------------------------------------------------------------------------------------------------------------------------------------------------------------------------------------------------------------------------------------------------------------------------------------------------------------------------------------------------------------------------------------------------------------------------------------------------------------------------------------------------------------------------------------------------------------------------------------------------------------------------------------------------------------------------------------------------------------------------------------------------------------------------------------------------------------------------------------------------------------------------------------------------------------------------------------------------------------------------------------------------------------------------------------------------------------------------------------------------------------|-------------------------------------------------------------------------------------------------------------------------------------------------------------------------------------------------------------------------------------------------------------------------------------------------------------------------------------------------------------------------------------------------------------------------------------------------------------------------------------------------------------------------------------------------------------------------------------------------------------------------------------------------------------------------------------------------------------------------------------------------------------------------------------------------------------------------------------------------------------------------------------------------------------------------------------------------------------------------------------------------------------------------------------------------------------------------------------------------------------|

- [24] D. R. Fiske, Phys. Rev. D **69**, 047501 (2004).
- [25] D. R. Fiske, Ph.D. thesis, University of Maryland, College Park (2004).
- [26] . T. Tsuchiya, G. Yoneda, and H. Shinkai, Phys. Rev. D **83**, 064032 (2011).
- [27] M. Alcubierre *et al.*, Classical Quantum Gravity **21**, 589 (2004).
- [28] G. Zumbusch, Classical Quantum Gravity **26**, 175011 (2009).
- [29] C. Bona and C. Bona-Casas, Phys. Rev. D **82** 064008 (2010).
- [30] V. Paschalidis, J. Hansen, and A. Khokhlov, Phys. Rev. D **78**, 064048 (2008).